Vehicle's Turning Time Span Estimation Based on Linear and Non-linear Computational Turning Model

Chenghao Li *

Department of Mechanical Engineering Dalian University of Technology Dalian 116033, China

* Corresponding Author Email: davidli2002@mail.dlut.edu.cn

Abstract. The time span of a vehicle making turns, which is from the time a turn starts to the time the turn ends, are the basis of determination of essential data of vehicle motion like slip angles, forces on tires, except the vehicle is in an ideal one-dimensional motion. When the road condition is sensed by sensors on vehicle's driver assistance systems, how to take a turn is the next step that should be calculated. After the turn starts, the end time of the turn should be adjusted in real time to remedy the imperfection digital simulation of the road sensed by the sensors. This paper compares two turning models and proposes an algorithm to adjust the end time of the turning time span during the turning motion of the vehicle. Subsequently, the algorithm is applied to two classic models of car, BMW M3 and Chevrolet Cavalier in four common motions: U-turn, lane change, sharp U-turn and sharp lane change. The algorithm proposed can be applied to every scenario that should take use of the turning time length, including the mathematical model of crossings, traffic flow of rush hours, or simply estimate the time span in unmanned vehicle control systems.

Keywords: Vehicle; U-turn; lane change; model prediction control for vehicle; turning time.

1. Introduction

One of the targets that unmanned vehicle systems are trying to achieve is to ensure the smoothness of the traffic. Every turn and lane change may lead to a fluctuation in the traffic system as a whole, and every variable in the turning motion of a vehicle should be constrained under a controllable, safe condition. As early as 1987, tire model regarding with physics formula was enormously improved by Egbert Bakker, Lars Nyborg and Hans B. Pacejka, taking the slide force, the self-aligning torque's change with brake force, and influences of vertical load, camber into consideration [1]. Xiaodong Wang concludes that U-turning vehicles consume more of the available green time and more of the lane's available capacity than left-turning vehicles [2], but he only gives the conclusion under the mathematical basis, without considering the mechanical availability. Similarly, Pan Liu estimated the critical gaps and follow-up time for U-turn movement at unsignalized intersections [3]. Jun-qiang L, et al researched on the travel time of left-turning vehicles at signalized intersection, succeeded in drawing the conclusion about the relationship of the opposing through flow rate and the vehicle's travel time [4]. M3 distribution, according to them, overrides Poisson distribution when it comes to applicable scope and performance as a whole. Poisson distribution. Damrongrit (Neng) Piyabongkarn et al establishes an algorithm for estimation of slip angle in an economical way based on kinematics, discussing the safety limits of slip angle and the range of it in a certain span of turn [5], which generates a limitation when the vehicle is in a turn. Guillaume Baffet, Ali Charara and Joanny Ste´phant establishes a simulation of the road friction on vehicle's tire based on single-track model without considering the large lateral acceleration [6], but it can neither be applied when a vehicle's turn needs to be completely simulated, nor estimates the turning time domain. Metzler M., Tavernini D., Sorniotti A. and Gruber P. have designed an explicit nonlinear model predictive control (ENMPC) considering the yaw and lateral stability of a vehicle [7]. Also, ENMPC is used in the antilock braking system (ABS) in [8]. The quantile regression forests method is used by C. Wissing, T. Nattermann, K. Glander and T. Bertram to predict the remaining time of a lane change maneuver, whose result can be taken into account as a reference for driving strategy [9]. The synthesized safety distance for lane changing (SSDLC), which is the weighted sum of the lane changing safety distance and the traditional safety distance, is studied by Jiayu Fan, Jun Liang and Anjan K. Tula, calculating the

appropriate lane changing time point [10]. A linear time-varying model predictive control (LTV MPC) controller of low order is built by Paolo Falcone, Francesco Borrelli et al to stabilize the vehicle taking slip angle into consideration [11].

Previous researches all have their own pros and cons, but most of their researches focus on either a mathematical problem about the influence of a vehicle's turn in traffic, or various safety conditions and variables estimation under a certain mechanical model. However, a time domain of a turn under a mechanical model is needed to provide a more accurate time estimation for mathematical model. A different time span of turn may lead to a metabolic situation for a single turn, which may affect not only traffic problems, but also the vehicle's motion and driver's safety.

This study presents an adaptive algorithm to specify the turning time span and the optimization of the end time of turn in real time, including lane changes and U-turns. It is vital for not only the application in self-driving technology, but also the future research about the slip angle, road-tire friction model, vehicle stability control, pedestrian safety, road intersection safety, active safety system, etc.

2. Mechanism

2.1. Nomenclature

x Longitudinal fixed x-y axis of vehicle.
y Lateral fixed x-y axis of vehicle.
χ Orientation of the vehicle.
δ Turn angle (difference between tire orientation and vehicle orientation).
R Rotational matrix.
a Length from the vehicle's center of mass to the front tire.
b Length from the vehicle's center of mass to the rear tire.
m Mass of the vehicle.
α Slip angle.
I_z Yaw moment of inertia
$\vec{u}_1$ Unit vector whose direction is parallel with vehicle's orientation.
$\vec{u}_2$ Unit vector whose direction is orthogonal to vehicle's orientation.

2.2. Wheel Model

To estimate the time span for a vehicle when it is taking a turn, it is important to correctly set the model for the motion of the vehicle.

2.2.1. Two-wheel Simplified Model

Four tires of the vehicle are divided into two groups, front and rear. Suppose the force on left tires are the same as the one on right tires, respectively. Forces are orthogonal with the tire's heading direction. Rear tires are in the same direction as the vehicle's orientation. Since under this assumption, the forces on both sides are regarded as the same, the force due to left and right wheels can be replaced by the sum acting on a center 'virtual wheel':

$$\vec{F}_{center} = \vec{F}_{left} + \vec{F}_{right} \tag{1}$$

The existence of these two virtual wheels means that this paper doesn't take Ackermann angle into consideration.

2.2.2. Front Virtual Center Wheel

Set part *i* to be any part of the vehicle, and the position vector $\vec{r}_i = \vec{r}_G + \vec{r}_P$ where $\vec{r}_P = l_i \begin{pmatrix} cos\chi \\ sin\chi \end{pmatrix}$ and l_i is a constant.

Thus,

$$\vec{v}_i = \vec{v}_G + l_i\chi' \begin{bmatrix} -sin\chi \\ cos\chi \end{bmatrix} \tag{2}$$

Since the front tire is at positive position relative to the center of mass, the relative velocity can be denoted as:

$$\int_0^a \chi' \begin{bmatrix} -sin\chi \\ cos\chi \end{bmatrix} dl = a\chi' \begin{bmatrix} -sin\chi \\ cos\chi \end{bmatrix} \tag{3}$$

The relation between the velocity of the front tire, $\vec{v}_f$, and the velocity of the center of mass of the vehicle, $\vec{v}_G$, is:

$$\overrightarrow{v_f} = \vec{v}_G + a\chi'\vec{u}_2 \tag{4}$$

2.2.3. Rear Virtual Center Wheel

Since the rear tire is at negative position relative to the center of mass, the relative velocity can be denoted as:

$$\int_0^{-b} \chi' \begin{bmatrix} -sin\chi \\ cos\chi \end{bmatrix} dl = -b\chi' \begin{bmatrix} -sin\chi \\ cos\chi \end{bmatrix} \tag{5}$$

The relation between the velocity of the rear tire, $\vec{v}_r$, and the velocity of the center of mass of the vehicle, $\vec{v}_G$, is:

$$\overrightarrow{v_r} = \vec{v}_G - b\chi'\vec{u}_2 \tag{6}$$

2.3. Motion Model

2.3.1.Slip Angle

No matter what kind of models are applied, slip angle is indispensable.

(1) Turn Angle

The difference between the orientation of the vehicle and the orientation of the tire may play the vital role in the process of the turn. The trajectory is basically determined by the turn angle. The maximum turn angle varies with different types of vehicles.

For U-turn:

$$\delta = \begin{cases} 0 & t < t_{start} \\ \frac{\delta_0}{2}\left[1 - \cos\frac{\pi(t - t_{start})}{t_0}\right] & t_{start} \le t < t_{start} + t_0 \\ \delta_0 & t_{start} + t_0 \le t < t_{end} \\ \frac{\delta_0}{2}\left[1 - \cos\frac{\pi(t_{end} + t_0 - t)}{t_0}\right] & t_{end} \le t < t_{end} + t_0 \\ 0 & t_{end} + t_0 \le t \end{cases} \tag{7}$$

(8) Is the process of a simple, complete U-turn? In this model, t_{start} and t_{end} is the time that the turn begins and completes. δ_0 is the greatest angle that the vehicle's front tire that can be achieved. t_0 is the time span that the tire turns from the original orientation to the greatest angle orientation. Take data in TABLE I as an example:

Table I. Motion Data Sample.

Start time (s)	δ_0 (rad)	t_0 (s)	End time (s)
1	0.1	2	8

The ideal turning time span is 9 seconds in this case, from t=1s to t=10s. Fig. 1 demonstrates the changing process of the turning angle.

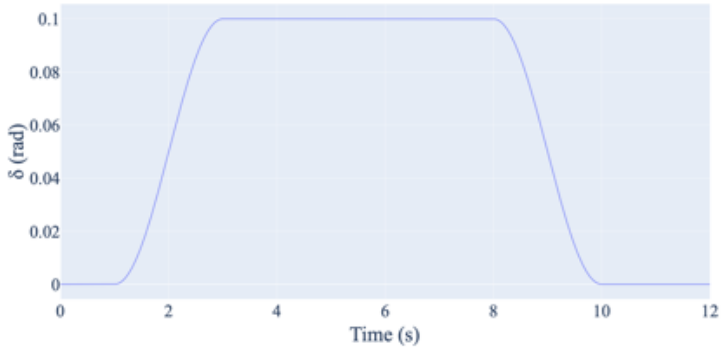


Figure 1. Turn Angle's Change with Time (U-Turn).

For lane change:

$$\delta = \begin{cases} 0 & t < t_{start} \\ \delta_0 \sin\left(\dfrac{t - t_{start}}{t_0}\right) & t_{start} \le t < t_{start} + 2\pi t_0 \\ 0 & t_{start} + 2\pi t_0 \le t \end{cases} \quad (8)$$

(8) Is the process of a simple, complete lane change? The lane change process is described in a sinusoidal function. Fig. 2 is the sample plot of the motion data sample in Table II.

Table II. Motion Data Sample.

Start time (s)	δ_0 (rad)	t_0 (s)	End time (s)
1	0.1	$\frac{1}{2\pi}$	2

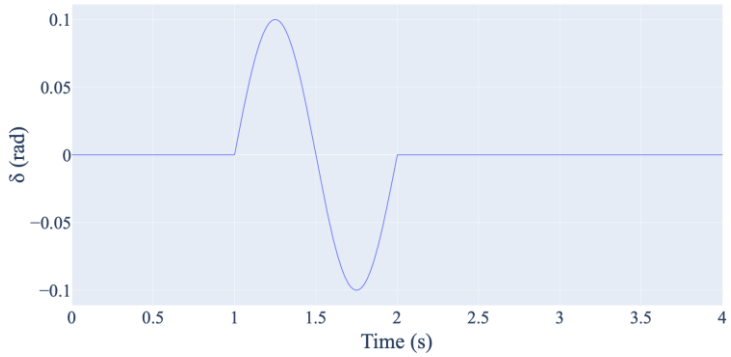


Figure 2. Turn Angle's Change with Time (Lane Change).

(2) Slip Angle

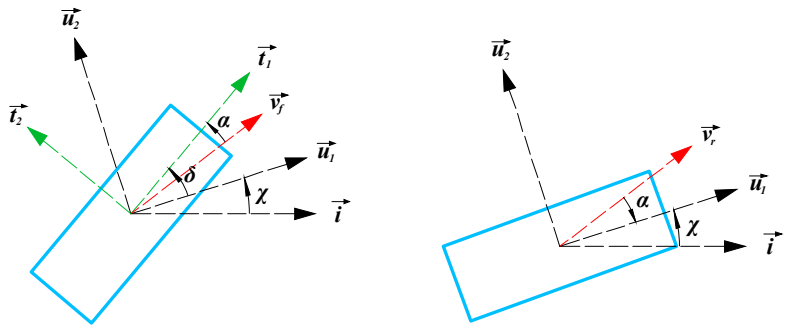


Figure 3. Sketch of the Vehicle's Orientation.

According to the Fig. 3:

$$\alpha_f = \delta - \sin^{-1}\frac{\vec{v}_f \cdot \vec{u}_2}{\|\vec{v}_f\|} \tag{9}$$

$$\alpha_r = -\sin^{-1}\frac{\vec{v}_r \cdot \vec{u}_2}{\|\vec{v}_r\|} \tag{10}$$

2.4. Weight Forces

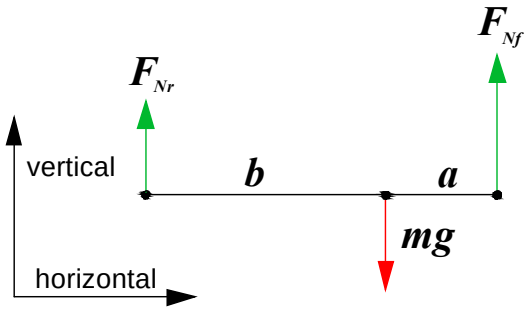


Figure 4. Sketch of the Lateral View of the Vehicle.

According to Fig. 4, the vertical weight forces that are needed by both linear and nonlinear turning model is calculated like this:

$$\begin{cases} mg = F_{N_f} + F_{N_r} \\ \mathrm{aF_{N_f}} - bF_{N_r} = 0 \end{cases} \tag{11}$$

And the weight forces on front and rear tire are like this:

$$F_{N_f} = \frac{b}{a+b}mg \tag{12}$$

$$F_{N_r} = \frac{a}{a+b}mg \tag{13}$$

2.5. Linear Turning Model

2.5.1. Linear turning model has the simplest formula, since the slip angle using in the linear model should be less than 4°, which means that no matter how α changes, its value is approximately near the α value itself:

$$F = C\alpha \tag{14}$$

Where *C* is the corning stiffness of the tire, which varies at different tire positions, front or rear. According to (14):

$$F_f = C_f\alpha_f \tag{15}$$

$$F_r = C_r\alpha_r \tag{16}$$

2.5.2. Torque on Rear Virtual Tire

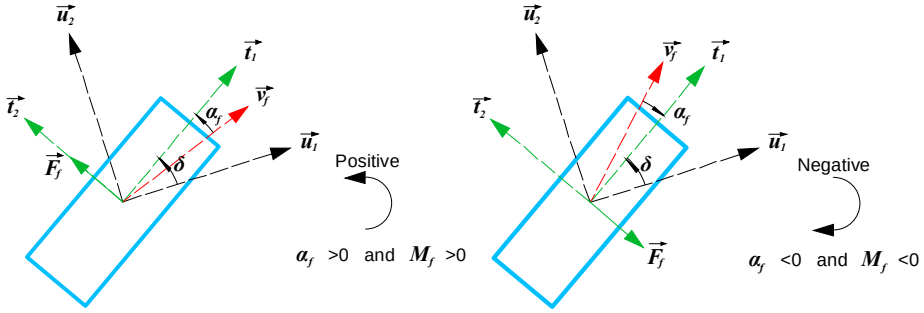


Figure 5. Sketch of the Tire Force and Orientation.

According to Fig. 5, rear virtual tire has no turn angle since its orientation is the same as the vehicles, thus:

$$M_r = -b\|F_r\| \tag{17}$$

2.5.3. Torque on Front Virtual Tire

$$M_f = aC\alpha_f \cos\delta \tag{18}$$

2.6. Nonlinear Turning Model

2.6.1. Force model

$$F = Ctan(\alpha)f(\lambda) \tag{19}$$

Where

$$f(\lambda) = \begin{cases} (2-\lambda)\lambda \\ 1 \end{cases} \tag{20}$$

Where

$$\lambda = \left|\frac{\mu F_N}{2Ctan(\alpha)}\right| \tag{21}$$

Where F_N is the vertical force acting on tire.

λ is a required variable that must be used for nonlinear turning model.

$$\lambda_f = \left|\frac{\mu F_{N_f}}{2Ctan(\alpha)}\right| \qquad \lambda_r = \left|\frac{\mu F_{N_r}}{2Ctan(\alpha)}\right| \tag{22}$$

2.6.2. Torque on virtual tires

When applying the nonlinear model, the torque on rear virtual tire stays the same as the one when applying linear model, like (17), because there is no angle magnitude for the rear angle. However, when it comes to the front tire, α should be taken into consideration.

$$M_f = F_f a = aCtan(\alpha)f(\lambda) \tag{23}$$

2.7. Application of Linear and Nonlinear Turning Model

For a BMW M3, when applying (15), (16), (19), (20), (21), (22), the force condition is demonstrated in Fig. 6.

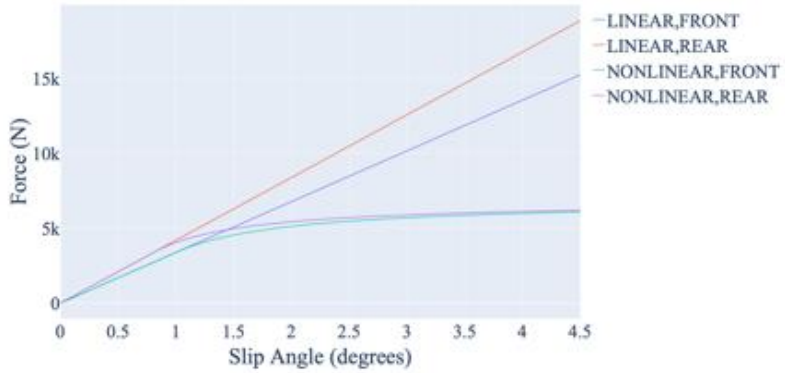


Figure 6. Force Estimation Comparison of the Linear and Nonlinear Model on BMW M3's Front and Rear Tire.

The greatest difference of these two models is the condition decided by the magnitude of the angle. When α becomes larger, the linear model tends to overestimates the magnitude of the force, as is shown in Fig. 6. However, linear model may give a faster calculation and less power or time for calculating.

2.8. Motion Matrix

To apply the turning model above, BMW M3 and Chevrolet Cavalier, whose basic information is listed in TABLE III and TABLE IV, are used to demonstrate the turning process.

TABLE III. Basic Statistics of BMW M3.

vehicle model	BMW M3
frictional coefficient	0.9
front tire corning stiffness	194000 N/rad/axle
rear tire corning stiffness	240000 N/rad/axle
front tire to center of mass	1.36 m
rear tire to center of mass	1.37 m
mass	1549 kg
yaw moment of inertia	2886 kg·m^2

Table IV. Basic Statistics of Chevrolet Cavalier.

vehicle model	Chevrolet Cavalier
frictional coefficient	0.9
front tire corning stiffness	58000 N/rad/axle
rear tire corning stiffness	58000 N/rad/axle
front tire to center of mass	0.98 m
rear tire to center of mass	1.66 m
mass	1187 kg
yaw moment of inertia	1928 kg·m^2

To express the motion situation of the vehicle, a matrix is generated.

$$mm = \begin{bmatrix} x \\ y \\ \chi \\ x' \\ y' \\ \chi' \end{bmatrix} \tag{24}$$

Thus, the initial motion condition is denoted by mm_0 matrix as:

$$mm_0 = \begin{bmatrix} x_0 \\ y_0 \\ \chi_0 \\ x_0' \\ y_0' \\ \chi_0' \end{bmatrix} \tag{25}$$

Thus, the problem turns into an initial value problem. *solve_ivp* imported from *scipy. integrate* is used as the solver. See Appendix I.

Before applying the solver, *motion_matrix* should be defined:

$$mm' = \begin{bmatrix} x' \\ y' \\ \chi' \\ x'' \\ y'' \\ \chi'' \end{bmatrix} \tag{26}$$

x', y', χ' are directly given in the last three elements in *mm* matrix.

$$x'' = \frac{-F_f \sin(\delta + \chi) - F_r \sin(\chi)}{m} \tag{27}$$

$$y'' = \frac{F_f \cos(\delta + \chi) + F_r \cos(\chi)}{m} \tag{28}$$

$$\chi'' = \frac{aF_f cos\delta - bF_r}{I_z} \tag{29}$$

2.9. Application of the motion matrix

With the timer starting, the turn starts at the condition ofmm_0. When *t* increases, δ changes, according to (7) and (8). Then the slip angle is determined together with$\overrightarrow{u_2}$, according to (9) and (10). χ is given in mm0, and the corresponding mm matrix after the turn starts. Thus, the trajectory of the vehicle can be calculated with the time going on, because the x coordinate and the y coordinate are both known in the mm matrix.

Take BMW M3 as example, suppose the vehicle starts its turn at the origin, x=0 and y=0. The tire-road friction index μ=0.8. Since the turn hasn't start yet, chi value is also 0. The vehicle is moving ahead in a speed of 30 miles per hour, whose direction is +x, then:

$$mm_0 = \begin{bmatrix} 0 \\ 0 \\ 0 \\ 30 \\ 0 \\ 0 \end{bmatrix} \tag{30}$$

As the vehicle starts the turn, the wheel starts to rotate, which means δ is changing. Whether the vehicle has finished the turn depends on the tendency of χ.

Under this circumstance, velocity of the center of mass of the vehicle can be directly denoted as:

$$v_{center\ of\ mass} = \begin{bmatrix} x' \\ y' \end{bmatrix} \tag{31}$$

When the vehicle is making a U-turn, the goal is to make sure χ turns to 180˚ after it starts getting greater, as is shown in Fig. 6.

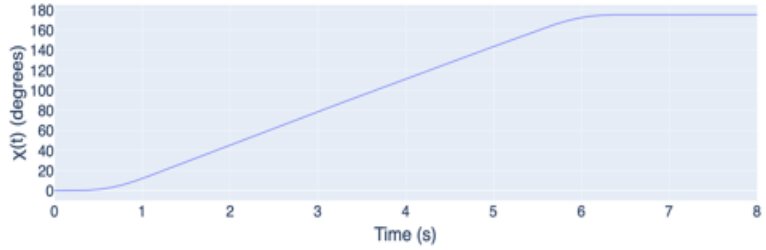


Figure 7. U-Turning BMW M3's Orientation Changing with Time (Linear Model).

And the trajectory condition of the vehicle is shown in Fig. 7.

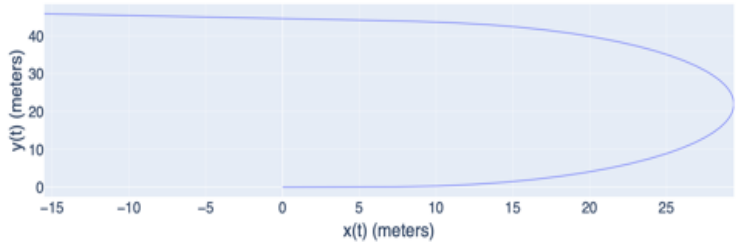


Figure 8. Trajectory of the BMW M3 in Fig. 6 (Linear Model)

When the vehicle is making a lane change, the goal is to make sure that χ is back to 0˚ again after it is greater than zero, as is shown in Fig. 9

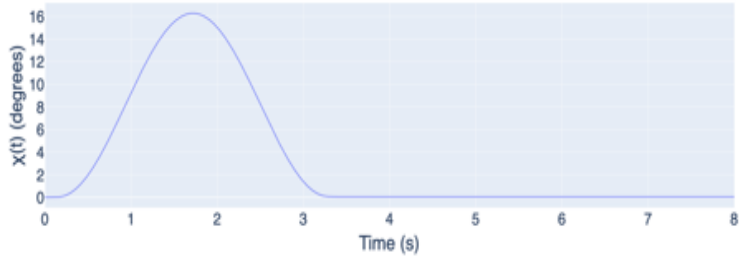


Figure 9. Lane Changing BMW M3's Orientation Changing with Time (Linear Model).

And the trajectory condition of the vehicle is shown in Fig. 10.

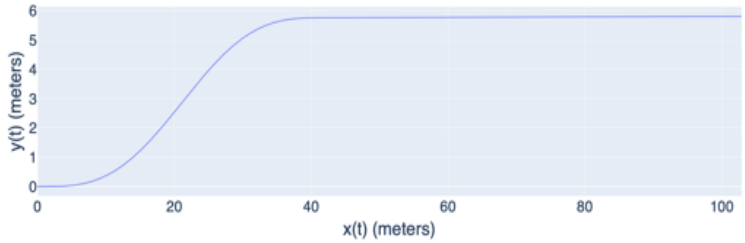


Figure 10. Trajectory of the BMW M3 in Fig. 9 (Linear Model).

2.10. End time estimation

All of the motion variables that are taken into consideration are able to be included in the tire model and the motion matrices during the process of the whole turn. In Fig. 1 and Fig. 2, the end time is already set and is a constant number. Set the end time as a variable, and keep refreshing the end time every *dt* second(s). At the same time, keep monitoring the χ value. As soon as χ satisfies the turn-end condition, stop refreshing the end time, and output it. *dt* can be determined by the requirement of the accuracy of the time span needed. In the U-turn case above, the ending time should be about 4.30 seconds when taking *dt* as 0.01s.

2.10.1. End time with vehicle length (U-turn)

According to (12) and (13), the length of the vehicle, no matter the length between the front tire of the vehicle and the center of mass (*a*) or the one between the rear tire of the vehicle and the center

of mass (*b*), are related to the vertical forces. When the length increases, the ending time tend to increases. mm_0 of Fig. 11 and Fig. 12 is in (30), and the motion data in TABLE V.

Table V. Motion Data Sample.

Start time (s)	δ_0 (rad)	t_0 (s)	End time (s)
0.1	$\frac{\pi}{12}$	1	TBD

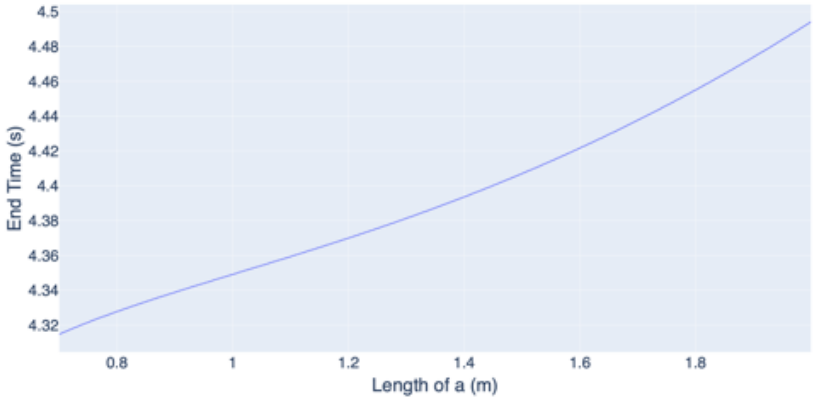


Figure 11. *a* versus end time for U-turn.

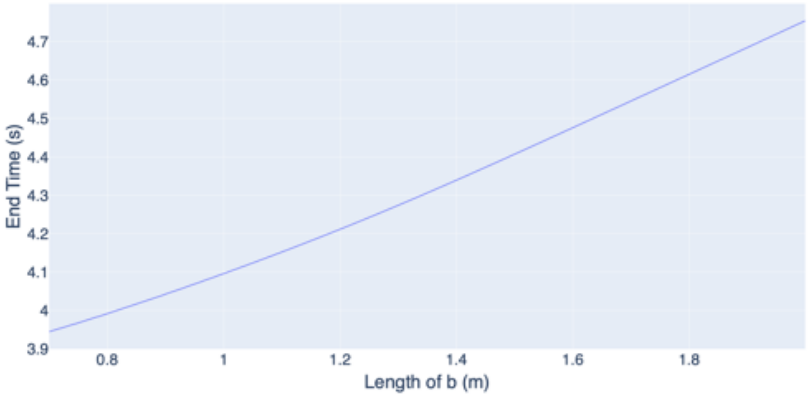


Figure 12. *b* versus end time for U-turn.

2.10.2. End time and the load of the vehicle (U-turn)

According to [12], with the load of the vehicle increases, the cornering stiffness of the vehicle may make a difference. The mass of the load can be viewed as the variation of the mass of the vehicle. Thus, when the mass of the vehicle varies, the end time may also vary, as is shown in FIG 14 and FIG 15.

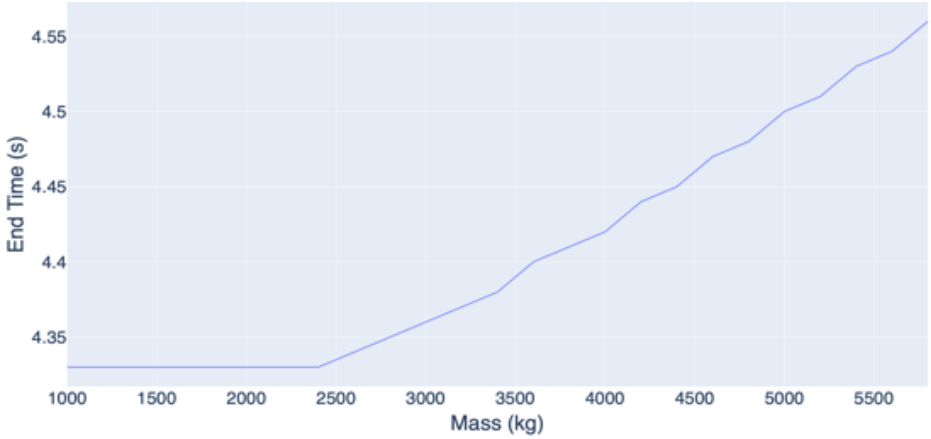


Figure 13. Aass of the vehicle versus end time for U-turn.

2.11. Possible Extensions

Lane changing process is different from the U-turn, since the end time is not serving as an influencing factor of the time span. Since lane change, different from U-turn's 180˚, the motion is related to the width of the lane. It is not rigorous to directly apply this algorithm.

The process of estimating the ending time of a turn, or several continuous turns, are all based on the wheel's turning angle stays the same, which means δ_0 and the t_0 stays the original turn, (7) and (8) are not changed. However, when a turn has to be ceased, that must because the turn should not be taken as the original condition. Thus, when the turn angle and corresponding t_0 are modified, the algorithm and the model may not work properly.

3. Conclusion

This paper has compared the difference between two different turning models, linear model and nonlinear model, when a vehicle is in two kinds of motion, U-turn and lane change. When the slip angle is an angle whose tan (α) can be approximated as α, linear works. However, when the turn is sharp, no matter U-turn or lane change, linear model may give an approximation whose error is unacceptable. According to the turning model, the posture of the vehicle was simulated in a given time span. Subsequently, according to the change of the posture, and the fixed start time, the ending time was computed in real time. Two vehicle models are applied to the algorithm, BMW M3 and Chevrolet Cavalier. This time estimation is based on the vehicle's engineering model, serving as a more accurate tool for future studies. When researching on the traffic problem or urban planning concerning about the crossings, this algorithm may provide a more accurate scene when making a mathematical model.

The real time accurate ending time guaranteed the completeness of the turn, making the vehicle's actual posture approaching as much as possible to the ideal situation. However, the evaluation raised by this paper only includes the consideration about the time change. As a matter of fact, when the vehicle is taking a turn that is not ideal, not only the motion variables mentioned in this paper change. Further, if Ackermann angle is taking into consideration, which means that the Two-wheel Simplified Model fails, the evaluation fails.

4. Appendix

I

```
soln = solve_ivp(
                motion_matrix,t_span,
                    (mm0[0],mm0[1],mm0[2],mm0[3],mm0[4],mm0[5]),
                    t_eval = times,
                    dense_output = True,
                    args=(car,forceType,turn),
                    rtol = 1e-6,
                    atol = 1e-6
                )
```

References

[1] Egbert Bakker, Lars Nyborg, and Hans B. Pacejka, "Tyre Modelling for Use in Vehicle Dynamics Studies." SAE International Congress and Exposition (1987) 0148-7191/87/0223-0421.

[2] Xiaodong Wang, "Effects of U-Turns on Capacity at Signalized Intersections and Simulation of U-Turning Movement by Synchro", Graduate Theses and Dissertations (2008).

[3] Pan Liu, "Evaluation of the Operational Effects of U -Turn Movement." PhD thesis, 2006.

[4] Leng Jun-qiang, Feng Yu-qin, Zhai Jing, Bao Lei, and He Yi. “Travel Time Model of Left-Turning Vehicles at Signalized Intersection.” Mathematical Problems in Engineering, vol. 2012, Article ID 473847.

[5] Damrongrit Piyabongkarn, Rajesh Rajamani, John A. Grogg, and Jae Y. Lew, “Development and Experimental Evaluation of a Slip Angle Estimator for Vehicle Stability Control.” IEEE Transactions on Control Systems Technology, vol. 17, no. 1 (2009): 78–88.

[6] Guillaume Baffet, Ali Charara, and Joanny Stephant. “Sideslip Angle, Lateral Tire Force and Road Friction Estimation in Simulations and Experiments.” 2006 IEEE Conference on Computer Aided Control System Design, 2006 IEEE International Conference on Control Applications, 2006 IEEE International Symposium on Intelligent Control, 2006, pp. 903-908.

[7] Davide Tavernini, Mathias Metzler, Patrick Gruber, and Aldo Sorniotti, “Explicit Nonlinear Model Predictive Control for Electric Vehicle Traction Control.” IEEE Transactions on Control Systems Technology, vol. 27, no. 4, pp. 1438-1451, July 2019.

[8] Davide Tavernini, Fabio Vacca, Mathias Metzler, Dzmitry Savitski, Valentin Ivanov, Patrick Gruber, Ahu Ece Hartavi, Miguel Dhaens, and Aldo Sorniotti, "An Explicit Nonlinear Model Predictive ABS Controller for Electro-Hydraulic Braking Systems", IEEE Transactions on Industrial Electronics, vol. 67, no. 5, pp. 3990-4001, May 2020.

[9] Christian Wissing, Till Nattermann, Karl-Heinz Glander, and Torsten Bertram. "Probabilistic Time-to-lane-change Prediction on Highways", 2017 IEEE Intelligent Vehicles Symposium (IV), 2017, 1452-457.

[10] Jiayu Fan, Jun Liang, and Anjan K. Tula, “A Lane Changing Time Point and Path Tracking Framework for Autonomous Ground Vehicle.” IET Intelligent Transport Systems, 2022.

[11] P. Falcone, F. Borrelli, H. E. Tseng, J. Asgari, and D. Hrovat. “Linear Time-Varying Model Predictive Control and Its Application to Active Steering Systems: Stability Analysis and Experimental Validation.” International Journal of Robust and Nonlinear Control 18, no. 8 (2008): 862–75.

[12] Goran S. Vorotovic, Branislav B. Rakicevic, and Sasa R. Mitic, Dragan D. Stamenkovic, “Determination of cornering stiffness through integration of a mathematical model and real vehicle exploitation parameters.”, FME Transactions (2013) 41, 66-71